
Real-Time Deepfake Detection in the Real-World

Bar Cavia Eliahu Horwitz Tal Reiss Yedid Hoshen

School of Computer Science and Engineering
The Hebrew University of Jerusalem, Israel

<https://vision.huji.ac.il/ladeda/>

{bar.cavia, eliahu.horwitz, tal.reiss, yedid.hoshen}@mail.huji.ac.il

Abstract

Recent improvements in generative AI made synthesizing fake images easy; as they can be used to cause harm, it is crucial to develop accurate techniques to identify them. This paper introduces "Locally Aware Deepfake Detection Algorithm" (*LaDeDa*), that accepts a single 9×9 image patch and outputs its deepfake score. The image deepfake score is the pooled score of its patches. With merely patch-level information, *LaDeDa* significantly improves over the state-of-the-art, achieving around 99% mAP on current benchmarks. Owing to the patch-level structure of *LaDeDa*, we hypothesize that the generation artifacts can be detected by a simple model. We therefore distill *LaDeDa* into *Tiny-LaDeDa*, a highly efficient model consisting of only 4 convolutional layers. Remarkably, *Tiny-LaDeDa* has $375 \times$ fewer FLOPs and is $10,000 \times$ more parameter-efficient than *LaDeDa*, allowing it to run efficiently on edge devices with a minor decrease in accuracy. These almost-perfect scores raise the question: is the task of deepfake detection close to being solved? Perhaps surprisingly, our investigation reveals that current training protocols prevent methods from generalizing to real-world deepfakes extracted from social media. To address this issue, we introduce *WildRF*, a new deepfake detection dataset curated from several popular social networks. Our method achieves the top performance of 93.7% mAP on *WildRF*, however the large gap from perfect accuracy shows that reliable real-world deepfake detection is still unsolved.

1 Introduction

Deepfake images are a leading source of disinformation with government and private agencies recognizing them as a grave threat to society (30; 45). Recent improvements in generative models, such as DALL-E (35), StableDiffusion (38), and Midjourney (2), significantly lowered the bar of creating fake images. Malicious parties are exploiting this technology to spread false information, damage reputations, and violate privacy online. Recent studies (6; 23; 18) showed that although deepfakes are semantically similar to real images, they have subtle, low-level artifacts that are easier to discriminate. This suggests that deepfake methods may gain from focusing on low-level image features.

We therefore introduce *LaDeDa*, a patch-based classifier that leverages local image features to detect deepfakes effectively. *LaDeDa*'s algorithm: i) splits an image into multiple patches ii) predicts a patch-level deepfake score iii) pools the scores of all image patches, resulting in the image-level deepfake score. To allow *LaDeDa* to work on small image patches, we use a variant of ResNet50 (21) that replaces some of the 3×3 convolutions by 1×1 convolutions. In particular, the best version of *LaDeDa* uses a receptive field of 9×9 , which we find is an effective size for deepfake image detection. This encourages the classifier to focus on local artifacts rather than global semantics. Using only patch-level information, *LaDeDa* significantly improves over the state-of-the-art (SoTA), achieving around 99% mAP on the most popular benchmarks.

Since LaDeDa focuses on small patches, we postulate that a very simple model may be sufficient for detecting deepfake artifacts. To test this hypothesis, we design Tiny-LaDeDa, a highly efficient model consisting of only 4 convolutional layers. We train Tiny-LaDeDa by performing logit-based distillation (22) using the patch-level deepfake scores predicted by LaDeDa (i.e., the teacher). Remarkably, Tiny-LaDeDa demonstrates superior computational efficiency compared to other SoTA methods (see Fig. 1), allowing efficient deepfake detection on edge devices with a minor decrease in accuracy.

With LaDeDa and Tiny-LaDeDa achieving an almost perfect score on current standard benchmarks, we ask whether deepfake detection is close to being solved. Arguably, the most popular source for spreading deepfakes is social media; we therefore test the performance of recent SoTA methods on deepfakes taken from social platforms. Perhaps surprisingly, we found that when using the current standard training protocols, SoTA methods (including ours) fail. Standard protocols attempt to simulate a real-world generalization, by training a detector using a single generative model (typically ProGAN (24)), and evaluate it across other generative models. However, the commonly used datasets in this simulation exhibit preprocessing discrepancies (e.g., real images are in lossy JPEG format while fake images simulated directly from a generator and saved in lossless PNG format), making the protocol less applicable for practical scenarios.

The failure in generalization to in-the-wild deepfakes persists even for methods that use post-processing augmentations that should make them robust to distribution shifts. To address these simulation imperfections, we introduce *WildRF*, a new deepfake detection dataset curated from popular social networks (Reddit, X (Twitter) and Facebook). *WildRF* serves as a comprehensive and realistic dataset that captures the diversity and complexities inherent in online environments, which includes varying resolutions, formats, compressions, editing transformations, and generation techniques.

We validate the effectiveness of *WildRF* by retraining current SoTA methods on it. Our method achieves the top performance of 93.7% mAP on *WildRF*. Notably, it generalizes across social media platforms (e.g., training on Reddit images and evaluating on Facebook images) and is robust to JPEG artifacts, despite not using post-processing augmentations during training. The evaluation on *WildRF* shows that there is still a large gap from perfect real-world deepfake detection and highlights the importance of using a real-world benchmark.

To summarize, our main contributions are:

1. Introducing *LaDeDa*, a state-of-the-art patch-based deepfake detector for the real-world.
2. Distilling *LaDeDa* into *Tiny-LaDeDa*, a fast and compact, yet accurate student model for deepfake detection on edge devices.
3. Introducing the *WildRF* benchmark, extending deepfake evaluation to real-world settings, which are currently lacking in popular simulated datasets.

2 Related work

Over the past few years, there has been a remarkable progress in generating photo-realistic images unconditionally (25; 14; 10; 48) or using text prompts (38; 36; 40). Deepfake detection aims to classify whether a given image was captured by a camera ("real") or generated via a generative model ("fake"). Two main paradigms exist to tackle this challenge.

Deepfake detection by supervised learning. These methods mostly focus on the architectural designs and discriminative features for discerning real and fake images. Wang et al. (43) proposed using ResNet50 as a deepfake classifier, trained on real and fake images from one GAN method,

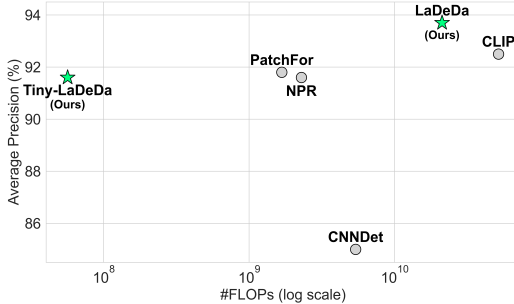


Figure 1: **Performance vs. efficiency trade-off.** Baselines comparison of average precision performance on real-world data as a function of floating-point operations per second (FLOPs) at inference time.

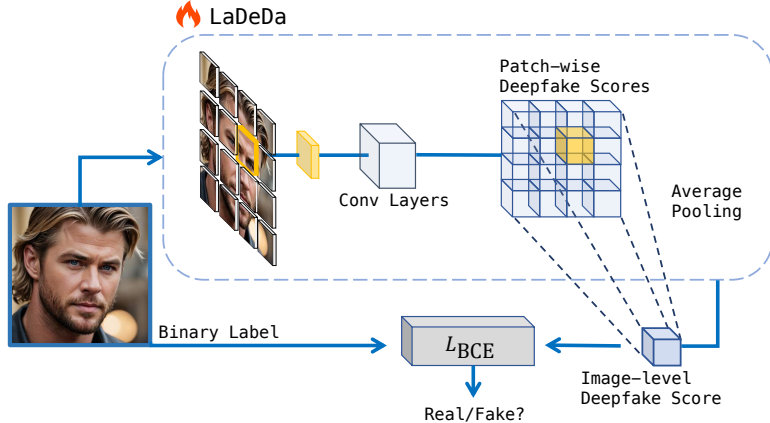


Figure 2: **LaDeDa Training**. By limiting its receptive field to $q \times q$ pixels, LaDeDa yields a deepfake score for each $q \times q$ patch. The image-level deepfake score is the global pooling of the patches scores. We use binary cross entropy loss between the image label and its deepfake score.

and evaluate the performance on other GAN methods. PatchFor (6) extends this idea, by learning a network that takes in a patch and outputs a deepfake score. While our method uses patches, similarly to PatchFor, we use knowledge distillation to estimate patch-level labels while PatchFor simply copies the image-level labels. Ojha et al. (32) leverages the pre-trained feature space of CLIP (34), by performing linear probing on CLIP’s image representations. Reiss et al. (37) introduced the concept of "fact checking" for detecting deepfakes, while being training-free and relying solely on off-the-shelf features.

Artifact-based detection methods These methods leverage inductive biases in the image preprocessing stage to discriminate between real and fake images. Marra et al. (28) revealed that GAN-based methods leave fingerprints in their generated images, which can be extracted using noise residuals from denoising filters. DIRE (44) focused on diffusion-based methods, measuring the error between an input image and its reconstruction, using a pre-trained diffusion model. Tan et al. (42) introduced the NPR (Neighboring Pixel Relationships) image representation, aiming to capture the local interdependence among image pixels caused by the upsampling layers in CNN-based generators.

3 Method

3.1 LaDeDa: Locally Aware Deepfake Detection Algorithm

Our core premise is that it is possible to discriminate between real and fake images with high accuracy based on low-level, localized features. This assumption is based on vast supporting literature (6; 23; 18; 17; 29; 47). We therefore introduce LaDeDa (denoted by ϕ), a model that maps patches p_i into a deepfake score $\phi(p_i)$, where higher values represent fake patches and lower values real ones.

Average pooling the patch-wise scores of all image patches results in the image-level deepfake score:

$$S(I) = \frac{1}{N} \sum_{i=1}^N \phi(p_i) \tag{1}$$

where I denotes the suspected image and p_1, p_2, \dots, p_N its patches.

LaDeDa is a variant of ResNet50 (21) (similar to BagNet (4)), but replaces most of the 3×3 convolutions by 1×1 ones, limiting the receptive field to $q \times q$ pixels (we use 9×9). The small receptive field forces LaDeDa to focus on local artifacts rather than global semantics, which we hypothesize is a good inductive bias for deepfake detection.

Specifically, for each image patch of size $q \times q$, LaDeDa infers a 2048-dimensional feature representation using multiple stacked ResNet blocks. The network applies a linear layer on the final patch-based representation, resulting in a per-patch score. The image-level score is the global pooling of the

per-patch scores. Finally, we apply a sigmoid activation on top of the image-level score resulting in the predicted likelihood that the image is fake. We optimize the network parameters using the binary cross entropy loss:

$$\mathcal{L} = - \sum_{f \in \mathcal{F}} \log(\sigma(S(f))) - \sum_{r \in \mathcal{R}} \log(1 - \sigma(S(r))). \quad (2)$$

where \mathcal{R} and \mathcal{F} denote the real and fake image datasets respectively, S denotes the network output (deepfake score) given an image, and σ is the sigmoid function. See Fig. 2 for LaDeDa illustration.

While our default choice is to pool the patch-level scores using global average pooling, it is also possible (and sometimes desirable) to use other pooling operations. For instance, using max pooling effectively classifies the image based on the most fake patch. Using average pooling, results in classifying the image based on the collective characteristics of all patches. These patch-based deepfake scores can yield an interpretable way to visualize the patches that contribute the most for LaDeDa classification decision (see Sec. 7). Additionally, the linearity of the average pooling operation, makes the architecture distillation-friendly, as we will elaborate on in Sec. 3.2.

Unlike many previous approaches that rely on prior knowledge from large-scale datasets (e.g., ImageNet (13)), LaDeDa randomly initializes its parameters and does not require pre-training. For further details on the LaDeDa’s architecture, see App. 9.1.

Relation to PatchFor (6). Both LaDeDa and PatchFor are patch-level methods, and must adapt to deepfake detection datasets that only provide image-level labels. PatchFor independently labels each patch based on the image label with equal weights i.e., all patches extracted from real images as equally real, and all patches extracted from fake images as equally fake. However, not all fake patches are easy to discriminate, and indeed, it is not necessary to correctly label the most difficult fake patches to obtain the correct overall image score. LaDeDa has the extra flexibility to provide adaptive importance to different patches, putting emphasis on the patches that are more discriminative.

3.2 Tiny-LaDeDa

Since LaDeDa operates on small patches, we hypothesize that a very simple model will suffice for detecting deepfakes. To this end, we propose Tiny-LaDeDa, a highly efficient model, obtained by distilling LaDeDa. As LaDeDa (i.e., the teacher) outputs patch-wise deepfake scores, we can train a simpler model (i.e., the student) to mimic the teacher’s knowledge; aiming for similar performance, while being much more compact. Specifically, we leverage logit-based distillation (22), which aims to transfer the knowledge encoded in the logit outputs (deepfake scores) of the teacher model to the student model.

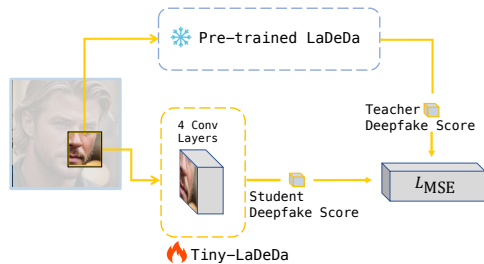
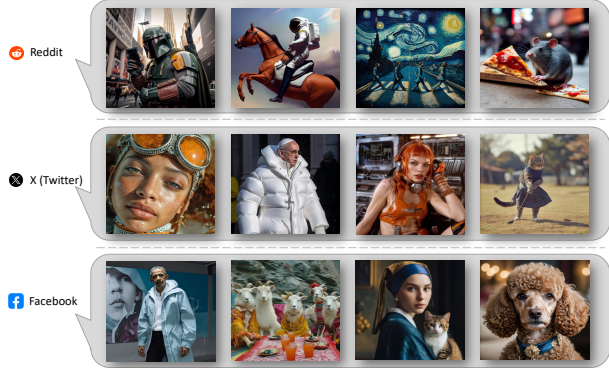


Figure 3: **Tiny-LaDeDa Distillation.** Pre-trained LaDeDa (teacher) transfers patch-level deepfake score knowledge to train Tiny-LaDeDa (student).

To train Tiny-LaDeDa, we use a trained LaDeDa model to generate a distillation training set comprising of samples in the form of $(p_i, \phi(p_i))$ for each patch p_i of each of LaDeDa’s training images. We then train Tiny-LaDeDa to predict a patch-wise logit (deepfake score), using the MSE loss between the student’s prediction and the teacher’s output (see Fig. 3). In logit-based distillation, the student is not limited by the teacher’s architecture. Consequently, Tiny-LaDeDa uses only 4 convolutional layers with 8 channels each, yielding a model 4 orders of magnitude smaller than the teacher. Similarly to LaDeDa, at inference time, Tiny-LaDeDa outputs an image deepfake score, by pooling per-patch deepfake scores. See App. 9.1 for further details on the Tiny-LaDeDa architecture.

4 Is the task of deepfake detection close to being solved?

When training and evaluating LaDeDa using commonly used deepfake detection benchmarks (32; 43), it achieves a near perfect score of 98.9% mAP, significantly outperforming the current SoTA (Tab. 1). This naturally raises the question: is the task of deepfake detection virtually solved? Essentially, deepfake detection methods must be effective in real-world scenarios. As a sanity check, we evaluated



Platform	Type	Years	#Images
Reddit	Real	2017-22	2150
	Fake	2022	2150
X (Twitter)	Real	2021-24	340
	Fake	2021-24	340
Facebook	Real	2021-24	160
	Fake	2021-24	160

Figure 4: **WildRF Overview.** A realistic benchmark consisting of images sourced from popular social platforms: *Reddit*, *X (Twitter)* and *Facebook*. WildRF contains high variability in a range of attributes including image resolutions, formats, semantic content, and transformations encountered *in-the-wild*.

them on a small sample of 10 images (5 real, 5 fake) taken from popular social networks (for a more comprehensive evaluation, see Sec. 5.1). Surprisingly, performance was near random, suggesting that the current evaluation protocol does not correlate with in-the-wild performance. We therefore reexamine the current evaluation protocols and suggest an alternative.

Current: simulated deepfake detection protocol. Most current methods follow a two-stage evaluation protocol. i) training a deepfake classifier using a set of "real" images and a set of "fake" images generated by a *single* generative model (typically ProGAN). ii) Evaluating the classifier on a set of real images and a set of generative models, most of which were not used for training. Many detection methods also use post-processing augmentations (e.g., JPEG compression, blur) during training to simulate unknown transformations an image may undergo before being encountered in-the-wild, potentially improving generalization. We refer to this as a *simulated* protocol.

Table 1: **Baseline performance on current (simulated) protocol.** mean average precision on 16 generative models from conventional benchmarks.

Method	mAP
CNNDet (43)	80.6
PatchFor (6)	94.9
CLIP (32)	96.3
NPR (42)	96.7
LaDeDa(Ours)	98.9

The simulated protocol is suboptimal. Common datasets used in the simulated protocol comprise real images sourced from standard datasets (e.g., LSUN (46), ImageNet (13)) in JPEG format (lossy compression), whereas the fake images are generated and saved in PNG format (lossless compression). Training a classifier on such datasets can introduce bias towards differences in compression, leading to inflated perceptions of generalization performance when evaluated on test sets with similar biases (see Sec. 5.1). Moreover, simulating real-world artifacts through augmentations may fail to capture the full diversity of corruptions encountered in practice (see Sec. 5.1). In App. 9.3.1 we provide further details on the commonly used datasets.

WildRF: Aligning deepfake evaluation with the real-world. We propose to improve deepfake evaluation and align it with the real-world by introducing *WildRF*, a realistic benchmark consisting of images sourced from popular social platforms. Specifically, we *manually* collected real images using keywords and hashtags associated with authentic, non-manipulated content (e.g., #photography, #nature, #nofilter, #streetphotography), and fake images using content related to AI-generated or manipulated visuals (e.g., #deepfake, #AIart, #midjourney, #stablediffusion, #dalle, #aigenerated). Our protocol is to train on one platform (e.g., Reddit) and test the detector on real and fake images from other unseen platforms (e.g., Twitter and Facebook). We denote this protocol as *social*. As both train and test data contain the type of variations seen in-the-wild, WildRF is a faithful proxy of real-world performance. See Fig. 4 for a WildRF overview.

Table 2: **Baseline performance - simulated protocol.** All methods are trained on ForenSynth train set (ProGAN), and evaluated on 16 generative models: (top) ForenSynth test set (43), and (bottom) UFD test set (32).

Method	ProGAN		StyleGAN		StyleGAN2		BigGAN		CycleGAN		StarGAN		GauGAN		Deepfakes		Mean	
	ACC	AP	ACC	AP	ACC	AP	ACC	AP	ACC	AP	ACC	AP	ACC	AP	ACC	AP	ACC	AP
CNNDet (43)	100	100	73.4	98.5	68.4	98.0	59.0	88.2	80.7	96.8	80.9	95.4	79.3	98.1	51.1	66.3	74.1	92.7
PatchFor (6)	99.6	99.9	93.9	99.2	94.5	99.6	74.4	89.6	85.3	93.5	76.3	90.4	64.7	92.4	89.2	92.8	84.7	94.6
CLIP (32)	99.8	100	84.9	97.6	75.0	97.9	95.1	99.3	98.3	99.8	95.7	99.4	99.5	100	68.6	81.8	89.6	97.0
NPR (42)	99.8	100	96.3	99.8	97.3	100	87.5	94.5	95.0	99.5	99.7	100	86.6	88.8	77.42	86.2	92.5	96.1
LaDeDa(Ours)	100	100	100	100	100	100	90.1	96.5	98.9	99.8	93.7	99.7	91.0	99.2	68.1	95.6	92.7	98.9
Tiny-LaDeDa(Ours)	98.2	100	99.1	100	98.8	100	86.8	94.8	79.5	95.9	96.9	99.8	84.9	91.4	85.9	98.0	91.3	97.5

Method	DALLE		Glide_100_10		Glide_100_27		Glide_50_27		Guided		LDM_100		LDM_200		LDM_200_cfg		Mean	
	ACC	AP	ACC	AP	ACC	AP	ACC	AP	ACC	AP	ACC	AP	ACC	AP	ACC	AP	ACC	AP
CNNDet (43)	52.5	66.8	54.2	73.7	53.3	72.5	55.6	77.7	52.3	68.4	51.3	66.6	51.1	66.5	51.4	67.3	52.3	68.4
PatchFor (6)	89.4	95.5	92.4	97.4	88.7	94.7	90.1	95.6	72.7	83.7	92.7	97.6	98.3	99.9	96.9	97.8	90.2	95.2
CLIP (32)	87.5	97.7	78.0	95.5	78.6	95.8	79.2	96.0	70.0	88.3	95.2	99.3	94.5	99.4	74.2	93.2	82.2	95.7
NPR (42)	94.5	99.5	98.2	99.8	97.8	99.7	98.2	99.8	75.8	81.0	99.3	99.9	99.1	99.9	99.0	99.8	95.2	97.4
LaDeDa(Ours)	93.5	99.8	99.0	100	99.3	100	99.0	100	81.0	91.1	99.8	100	99.7	100	99.7	100	96.3	98.8
Tiny-LaDeDa(Ours)	80.2	98.4	98.5	99.9	98.8	99.9	98.9	100	76.2	87.8	99.4	100	99.3	100	99.1	99.9	93.8	98.2

Table 3: **Poor generalization to real-world data.** Performance of SoTA methods trained on ForenSynth-train (ProGAN), evaluated on WildRF. It shows that training on the standard dataset, instead of in-the-wild deepfakes, generalizes poorly to in-the-wild images.

Method	Reddit		Twitter		Facebook		Mean	
	ACC	AP	ACC	AP	ACC	AP	ACC	AP
CNNDet (43)	51.2	49.7	50.3	50.2	50.0	43.4	50.5	47.8
PatchFor (6)	63.9	74.0	47.8	51.3	68.2	75.3	60.0	66.9
CLIP (32)	60.2	66.9	56.8	63.0	49.1	44.4	55.4	58.1
NPR (42)	65.1	69.4	51.7	52.5	77.8	86.3	64.8	69.4
LaDeDa(Ours)	74.7	81.8	59.9	67.8	70.3	90.1	68.3	79.9
Tiny-LaDeDa(Ours)	72.3	77.8	59.6	64.8	70.9	86.4	67.3	76.3

5 Experiments

We compare to SoTA baselines e.g., PatchFor (6), CNNDet (43), CLIP (32) and NPR (42) on the standard metrics: classification accuracy (ACC) (*threshold* = 0.5), and average precision (AP).

5.1 LaDeDa performance under the current (simulated) protocol

We begin by comparing LaDeDa to the baselines using the current (simulated) protocol. For training, we use the standard train set of the ForenSynth dataset (43), which contains real images from LSUN (46), and fake images from ProGAN. For evaluation, we use 16 different generative models taken from the test sets of ForenSynth (43) and UFD (32). The results in Tab. 2 demonstrate that LaDeDa and Tiny-LaDeDa outperformed the other baselines in terms of mAP (98.9%, 97.5% respectively), and LaDeDa also outperformed the baselines in terms of mean ACC (92.7%). For more details on the ForenSynth and UFD datasets, see App. 9.3.1.

Poor generalization to real-world data. While methods trained on ProGAN achieve high performance on detecting deepfakes created by a large set of other image generators, they do not perform well when tested on real-world data. Specifically, we evaluate the baselines using our WildRF dataset (Sec. 4). The results in Tab. 3 show much lower performance than the test set of the simulated protocol. This gap highlights the limitations of the simulated protocol in estimating real-world performance.

JPEG compression bias. Many methods report their results on the simulated protocol (which is biased, see Sec. 4), with two detector variants: i) training with post-processing augmentations (e.g., JPEG compression, blur), and ii) training without these augmentations. We claim that the later variant, can be biased towards compression artifacts. To demonstrate this, we retrained the CNNDet and CLIP baselines on ForenSynth without JPEG and blur training augmentations. For NPR, we used its official released checkpoint that does not include augmentations. We then evaluated these detectors on 3000 StyleGAN images (1500 real, 1500 fake) from ForenSynth’s test set, where we JPEG-compressed only the fake images. This setup allows us to examine whether compressing fake images impacts their

Table 4: **JPEG compression bias.** Detectors train under the simulated protocol demonstrate lower performance when JPEG-compressing the test *fake* images. 100 JPEG quality = no compression, 70 JPEG quality = lowest quality.

Dataset	Quality	CNNDet (43)		CLIP (32)		NPR (42)		LaDeDa (Ours)	
		ACC	AP	ACC	AP	ACC	AP	ACC	AP
StyleGAN	JPEG 100	83.3	96.2	88.0	98.5	97.6	99.8	100	100
StyleGAN	JPEG 90	50.1	83.4	66.5	90.3	50.1	43.0	52.9	68.1
StyleGAN	JPEG 80	50.0	71.3	56.8	84.6	49.9	38.0	50.3	54.5
StyleGAN	JPEG 70	50.0	46.4	53.9	79.3	49.9	36.8	50.0	44.7

Table 5: **Baseline performance - social protocol.** All methods are trained on WildRF train set (Reddit) and tested on WildRF test set. The results show a remarkable improvement compared to those achieved when trained using the simulated protocol.

Method	Train Set	Reddit		Twitter		Facebook		Mean	
		ACC	AP	ACC	AP	ACC	AP	ACC	AP
CNNDet (43)	Reddit	75.4	86.8	71.4	84.1	70.6	83.5	72.5	85.0
PatchFor (6)	Reddit	87.8	94.3	81.6	91.4	77.1	90.3	82.2	91.9
CLIP (32)	Reddit	80.8	94.2	78.1	93.1	78.4	90.6	79.1	92.5
NPR (42)	Reddit	89.8	95.7	79.5	90.3	76.6	88.9	81.9	91.6
LaDeDa(Ours)	Reddit	91.8	96.0	83.3	92.8	81.9	92.6	85.7	93.7
Tiny-LaDeDa(Ours)	Reddit	84.5	92.4	82.3	91.7	80.7	90.4	82.5	91.6

classification as real ones. As shown in Tab. 4, the detectors’ ability to correctly classify fake images decreases as a function of the compression rate, even at a relatively low compression quality of 90. Although the augmentation variants attempt to improve generalization by simulating the unknown transformations an image may undergo, in practice, the simulation is suboptimal (see Tab. 3).

5.2 Real-world deepfake detection

LaDeDa performance under our (social) protocol. We retrained and evaluate all methods using our proposed WildRF dataset. The train set comprises (1200 real, 1200 fake) images from Reddit, and the test set comprises (750 real, 750 fake) different images from Reddit, (340 real, 340 fake) images from X (Twitter), and (160 real, 160 fake) images from Facebook. The results in Tab. 5 show that training on real data is much more accurate than on simulated data.

JPEG Robustness. Fig. 5b shows that LaDeDa is robust to a range of JPEG compression rates. Note that training our method on WildRF made it JPEG-robust without using post-processing augmentations during training.

5.3 Real-time deepfake detection

Some practical scenarios require deepfake detection to not only be accurate, but also computationally efficient for real-time inference at scale and on edge devices. Fast inference will only get more important as deepfake content continues to spread across online platforms. Here, we evaluate computational efficiency in terms of floating-point operations per second (FLOPs) and network latency (seconds). FLOPs are a hardware-independent measure of computational complexity, quantifying the total number of floating-point operations (addition, subtraction, multiplication or division) required for a single forward pass of a given model. Network latency measures the time it takes the model to process an input (e.g., an image) and output its prediction. Clearly, real-time deepfake detection needs low FLOPs and latency. We simulate a low resource environment, similar to a mid-range smartphone with a single CPU core, and 4GB RAM. Tab. 6 shows that Tiny-LaDeDa with only a mild degradation in performance compared to LaDeDa, is $375\times$ faster and $10,000\times$ more parameter efficient.

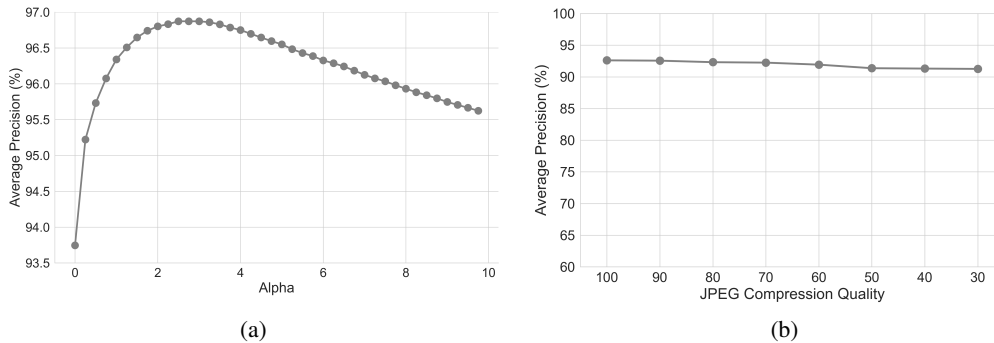


Figure 5: **(a) Local and global deepfake scores.** We show average precision (AP) performance on WildRF, when ensemble LaDeDa deepfake scores with CLIP (32) deepfake scores. **(b) JPEG robustness.** We show LaDeDa average precision (AP) performance on facebook test set, as a function of JPEG compression quality from 100 (no compression) to 30.

Table 6: **Real-time deepfake detection.** We show number of FLOPs, Parameters and Latency baselines comparison. In (red), we show the number relative to Tiny-LaDeDa, which demonstrates highly computational efficiency.

Method	#FLOPs	#Parameters	Latency
CNNDet (43)	5.40B ($\times 95$)	23.51M ($\times 18k$)	0.75 sec ($\times 37.5$)
PatchFor (6)	1.68B ($\times 30$)	0.191M ($\times 150$)	0.21 sec ($\times 10.5$)
CLIP(32)	51.89B ($\times 920$)	202.05M ($\times 15k$)	9.37 sec ($\times 470$)
NPR (42)	2.29B ($\times 40$)	1.44M ($\times 1.1k$)	0.35 sec ($\times 17.5$)
LaDeDa(Ours)	21.23B ($\times 375$)	13.64M ($\times 10k$)	2.87 sec ($\times 144$)
Tiny-LaDeDa(Ours)	0.0566B	0.00129M	0.02 sec

5.4 Local is all you need?

While LaDeDa achieves SoTA performance by focusing on local artifacts, we ask if global features provide complementary information. We thus linearly ensemble LaDeDa with the CLIP baseline (32), which trains a linear classifier on top of the semantic CLIP features. The resulting score is $S(I) = LaDeDa(I) + \alpha * CLIP_s(I)$ where I is an input image. The results in Fig. 5a show an increase of $\geq 3\%$ mAP on WildRF, when using the combined score, highlighting that global features are also useful for detecting deepfakes.

6 Ablation

Is distillation helpful? To test this, we trained Tiny-LaDeDa without distillation, using exactly the same data as LaDeDa (the teacher). It achieved decent accuracy on WildRF (mAP of 87.4%), but was worse than the larger LaDeDa model (mAP of 93.7%) and the distilled Tiny-LaDeDa (91.6%). We further trained Tiny-LaDeDa similarly to PatchFor (6), labeling each patch with its corresponding image-level label, achieving 84.5% mAP, which is 7% lower than when using LaDeDa’s estimated patch-level labels via distillation. We conclude that distillation is indeed helpful, however we see that a relatively simple model can already achieve good results.

Patch-size. LaDeDa’s effectiveness stems from its focus on local artifacts in small image patches. We evaluated LaDeDa using different receptive field patch sizes on WildRF. Fig. 6b shows that even with patches of size $q = 5$, LaDeDa can effectively discern between real and fake images, suggesting that small patches contain sufficient information for accurate deepfake detection.

Gradient inductive-bias. We investigate the inductive bias in terms of gradient-based patch representations (See Fig. 6a). LaDeDa achieves high performance even using raw pixels without any preprocessing, but a gradient-based representation generally works better. As we discuss in Sec. 7,

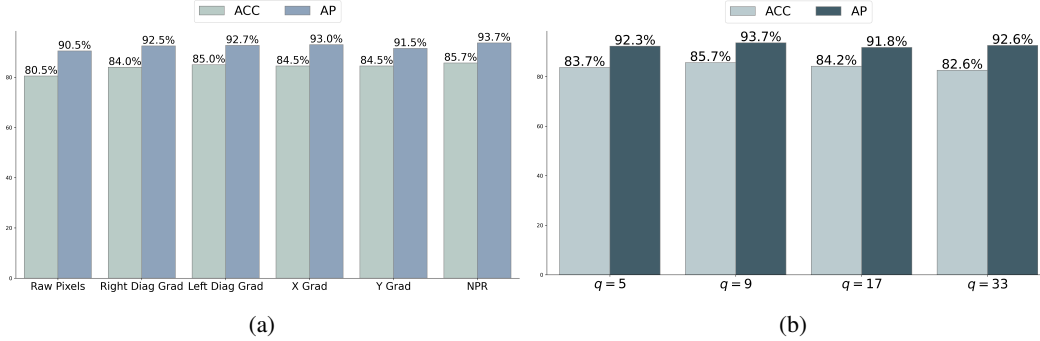


Figure 6: (a) *Image preprocessing* and (b) *patch-Size ablation*.

Table 7: *Pooling operator ablation*. LaDeDa test performance on ForenSynth, UFD and WildRF.

Method	Pooling	Test set					
		ForenSynth (43)		UFD (32)		WildRF	
		ACC	AP	ACC	AP	ACC	AP
LaDeDa	Max	90.1	99.1	88.9	97.0	84.9	92.4
LaDeDa	Average	92.7	98.9	96.3	98.8	85.7	93.7

this improvement can be attributed to gradients pointing up fine details and textures by focusing on changes in pixel values, effectively highlighting local discriminative features.

Pooling operator effectiveness. LaDeDa can use other pooling operations for image-level scoring beyond average pooling. Tab 7 shows the effectiveness of using max pooling i.e., the image-level deepfake score is the score of the most fake patch in it. It is slightly better in terms of AP on the ForenSynth test set, and worse on all other evaluation sets.

7 Discussion and limitations

Interpretability. Since LaDeDa maps each $q \times q$ patch into a deepfake score, we can create a heatmap visualizing the most discriminative patches. In Fig. 7a, we show two such heatmaps of fake images, where areas with notable intensity changes tend to get high deepfake scores. Delving into the most fake patches (patches with maximal deepfake scores), reveals that fake image patches appear smoother than those from real images (Fig. 7b). This aligns with studies (16; 11; 47) showing that generative models leave artifacts in high-frequency components due to the upsampling operation, making it difficult to synthesize realistic textures regions, thus smooth patches potentially smoother in fake images, and less smooth in real images, where a natural camera noise can appear.

Generalization to near and far deepfakes. When trained on a social network, our method and the baselines, generalize well to the other platforms. However, when trained on ProGAN/WildRF datasets the methods do not generalize well to the opposite dataset (WildRF/Simulated). To ensure that a single model can succeed on both protocols, we trained LaDeDa on a combination of 4k ProGAN train images and WildRF train set, achieving comparable results to train and evaluate separately on each protocol.

Size of WildRF. Although WildRF is a medium-sized dataset with around 5000 images, it is already sufficient for achieving high accuracy, likely due to the small scale of deepfake artifacts. While WildRF inevitably contains some biases, we expect these biases to reflect those encountered in real-world scenarios. Increasing the size and diversity of WildRF would likely further advance deepfake detection research.

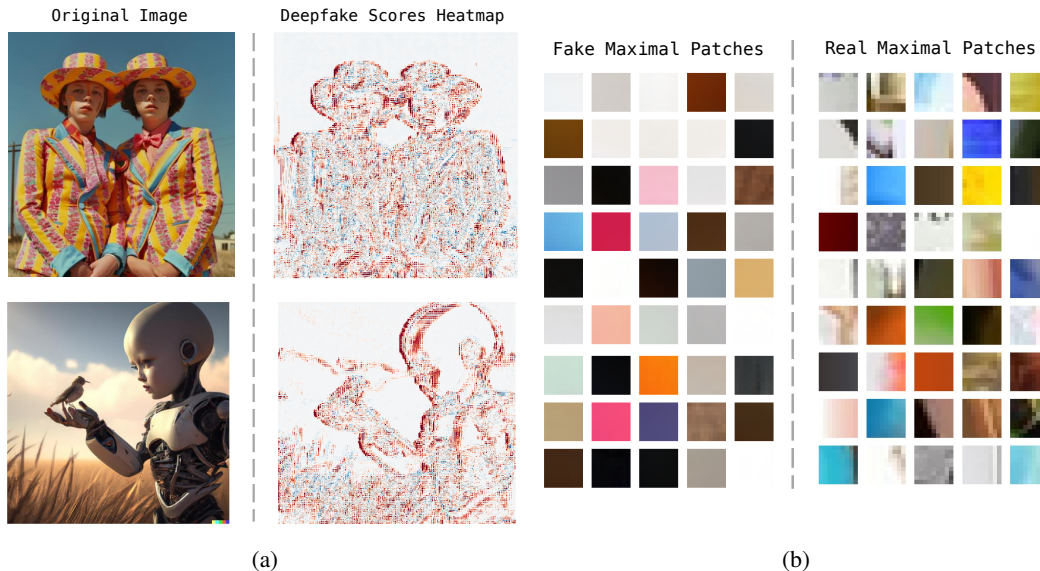


Figure 7: (a) *Deepfake score visualization*. High deepfake score in red, low deepfake score in blue. (b) *Maximal deepfake scores*. We show the most fake patches (i.e., patches with highest deepfake score) in fake and real images. It appears that the most fake patches are smoother in fake images, compared to the most fake patches in real images.

Broader Impacts. As deepfake content continues to spread across online platforms, effective detection methods are crucial for mitigating the risks of malicious usage. Our proposed approach offers a fast and accurate solution to address these threats.

8 Conclusion

We propose LaDeDa, a patch-based classifier that effectively detects deepfakes by leveraging local artifacts, and Tiny-LaDeDa, an efficient distilled version. Despite their high accuracy on current simulated benchmarks, we found that existing methods struggle to generalize to real-world deepfakes found on social media. To address this, we introduced *WildRF*, a new in-the-wild dataset curated from social networks, capturing practical challenges. While our method achieves top performance on WildRF, the considerable gap from perfect accuracy highlights that reliable real-world deepfake detection remains unsolved. We hope WildRF will drive future research into developing robust techniques against online disinformation that generalize to the real-world.

References

- [1] Lsun dataset. <https://github.com/fyu/lsun>. 15
- [2] Midjourney. <https://www.midjourney.com/home/>, 2022. 1, 15
- [3] <https://xihe.mindspore.cn/modelzoo/wukong>, 2022. 15
- [4] Wieland Brendel and Matthias Bethge. Approximating cnns with bag-of-local-features models works surprisingly well on imagenet. *arXiv preprint arXiv:1904.00760*, 2019. 3
- [5] Andrew Brock, Jeff Donahue, and Karen Simonyan. Large scale gan training for high fidelity natural image synthesis. *arXiv preprint arXiv:1809.11096*, 2018. 15
- [6] Lucy Chai, David Bau, Ser-Nam Lim, and Phillip Isola. What makes fake images detectable? understanding properties that generalize. In *Computer Vision—ECCV 2020: 16th European Conference, Glasgow, UK, August 23–28, 2020, Proceedings, Part XXVI 16*, pages 103–120. Springer, 2020. 1, 3, 4, 5, 6, 7, 8, 15
- [7] Chen Chen, Qifeng Chen, Jia Xu, and Vladlen Koltun. Learning to see in the dark. In *Proceedings of the IEEE conference on computer vision and pattern recognition*, pages 3291–3300, 2018. 15

- [8] Qifeng Chen and Vladlen Koltun. Photographic image synthesis with cascaded refinement networks. In *Proceedings of the IEEE international conference on computer vision*, pages 1511–1520, 2017. 15
- [9] Yiqun Chen and James Y Zou. Twigma: A dataset of ai-generated images with metadata from twitter. *Advances in Neural Information Processing Systems*, 36, 2024. 15
- [10] Yunjey Choi, Minje Choi, Munyoung Kim, Jung-Woo Ha, Sunghun Kim, and Jaegul Choo. Stargan: Unified generative adversarial networks for multi-domain image-to-image translation. In *Proceedings of the IEEE conference on computer vision and pattern recognition*, pages 8789–8797, 2018. 2, 15
- [11] Riccardo Corvi, Davide Cozzolino, Giovanni Poggi, Koki Nagano, and Luisa Verdoliva. Intriguing properties of synthetic images: from generative adversarial networks to diffusion models. In *Proceedings of the IEEE/CVF Conference on Computer Vision and Pattern Recognition*, pages 973–982, 2023. 9
- [12] Tao Dai, Jianrui Cai, Yongbing Zhang, Shu-Tao Xia, and Lei Zhang. Second-order attention network for single image super-resolution. In *Proceedings of the IEEE/CVF conference on computer vision and pattern recognition*, pages 11065–11074, 2019. 15
- [13] Jia Deng, Wei Dong, Richard Socher, Li-Jia Li, Kai Li, and Li Fei-Fei. Imagenet: A large-scale hierarchical image database. In *2009 IEEE conference on computer vision and pattern recognition*, pages 248–255. Ieee, 2009. 4, 5, 15
- [14] Prafulla Dhariwal and Alexander Nichol. Diffusion models beat gans on image synthesis. *Advances in neural information processing systems*, 34:8780–8794, 2021. 2
- [15] Prafulla Dhariwal and Alexander Nichol. Diffusion models beat gans on image synthesis. *Advances in neural information processing systems*, 34:8780–8794, 2021. 15
- [16] Ricard Durall, Margret Keuper, and Janis Keuper. Watch your up-convolution: Cnn based generative deep neural networks are failing to reproduce spectral distributions. In *Proceedings of the IEEE/CVF conference on computer vision and pattern recognition*, pages 7890–7899, 2020. 9
- [17] Joel Frank, Thorsten Eisenhofer, Lea Schönherr, Asja Fischer, Dorothea Kolossa, and Thorsten Holz. Leveraging frequency analysis for deep fake image recognition. In *International conference on machine learning*, pages 3247–3258. PMLR, 2020. 3
- [18] Robert Geirhos, Patricia Rubisch, Claudio Michaelis, Matthias Bethge, Felix A Wichmann, and Wieland Brendel. Imagenet-trained cnns are biased towards texture; increasing shape bias improves accuracy and robustness. *arXiv preprint arXiv:1811.12231*, 2018. 1, 3
- [19] Patrick Grommelt, Louis Weiss, Franz-Josef Pfrendt, and Janis Keuper. Fake or jpeg? revealing common biases in generated image detection datasets. *arXiv preprint arXiv:2403.17608*, 2024. 15
- [20] Shuyang Gu, Dong Chen, Jianmin Bao, Fang Wen, Bo Zhang, Dongdong Chen, Lu Yuan, and Baining Guo. Vector quantized diffusion model for text-to-image synthesis. In *Proceedings of the IEEE/CVF Conference on Computer Vision and Pattern Recognition*, pages 10696–10706, 2022. 15
- [21] Kaiming He, Xiangyu Zhang, Shaoqing Ren, and Jian Sun. Deep residual learning for image recognition. In *Proceedings of the IEEE conference on computer vision and pattern recognition*, pages 770–778, 2016. 1, 3
- [22] Geoffrey Hinton, Oriol Vinyals, and Jeff Dean. Distilling the knowledge in a neural network. *arXiv preprint arXiv:1503.02531*, 2015. 2, 4
- [23] Phillip Isola, Jun-Yan Zhu, Tinghui Zhou, and Alexei A Efros. Image-to-image translation with conditional adversarial networks. In *Proceedings of the IEEE conference on computer vision and pattern recognition*, pages 1125–1134, 2017. 1, 3
- [24] Tero Karras, Timo Aila, Samuli Laine, and Jaakko Lehtinen. Progressive growing of gans for improved quality, stability, and variation. *arXiv preprint arXiv:1710.10196*, 2017. 2, 14, 15
- [25] Tero Karras, Samuli Laine, and Timo Aila. A style-based generator architecture for generative adversarial networks. In *Proceedings of the IEEE/CVF conference on computer vision and pattern recognition*, pages 4401–4410, 2019. 2, 15
- [26] Diederik P Kingma and Jimmy Ba. Adam: A method for stochastic optimization. *arXiv preprint arXiv:1412.6980*, 2014. 14

- [27] Ke Li, Tianhao Zhang, and Jitendra Malik. Diverse image synthesis from semantic layouts via conditional imle. In *Proceedings of the IEEE/CVF International Conference on Computer Vision*, pages 4220–4229, 2019. 15
- [28] Francesco Marra, Diego Gragnaniello, Luisa Verdoliva, and Giovanni Poggi. Do gans leave artificial fingerprints? In *2019 IEEE conference on multimedia information processing and retrieval (MIPR)*, pages 506–511. IEEE, 2019. 3
- [29] Owen Mayer and Matthew C Stamm. Exposing fake images with forensic similarity graphs. *IEEE Journal of Selected Topics in Signal Processing*, 14(5):1049–1064, 2020. 3
- [30] National Security Agency. NSA, US Federal Agencies Advise on Deepfake Threats. <https://www.nsa.gov/Press-Room/Press-Releases-Statements/Press-Release-View/Article/3523329/nsa-us-federal-agencies-advise-on-deepfake-threats/>, 2023. 1
- [31] Alex Nichol, Prafulla Dhariwal, Aditya Ramesh, Pranav Shyam, Pamela Mishkin, Bob McGrew, Ilya Sutskever, and Mark Chen. Glide: Towards photorealistic image generation and editing with text-guided diffusion models. *arXiv preprint arXiv:2112.10741*, 2021. 15
- [32] Utkarsh Ojha, Yuheng Li, and Yong Jae Lee. Towards universal fake image detectors that generalize across generative models. In *Proceedings of the IEEE/CVF Conference on Computer Vision and Pattern Recognition*, pages 24480–24489, 2023. 3, 4, 5, 6, 7, 8, 9, 14, 15
- [33] Taesung Park, Ming-Yu Liu, Ting-Chun Wang, and Jun-Yan Zhu. Semantic image synthesis with spatially-adaptive normalization. In *Proceedings of the IEEE/CVF conference on computer vision and pattern recognition*, pages 2337–2346, 2019. 15
- [34] Alec Radford, Jong Wook Kim, Chris Hallacy, Aditya Ramesh, Gabriel Goh, Sandhini Agarwal, Girish Sastry, Amanda Askell, Pamela Mishkin, Jack Clark, et al. Learning transferable visual models from natural language supervision. In *International conference on machine learning*, pages 8748–8763. PMLR, 2021. 3
- [35] Aditya Ramesh, Mikhail Pavlov, Gabriel Goh, Scott Gray, Chelsea Voss, Alec Radford, Mark Chen, and Ilya Sutskever. Zero-shot text-to-image generation. In *International conference on machine learning*, pages 8821–8831. Pmlr, 2021. 1, 15
- [36] Aditya Ramesh, Prafulla Dhariwal, Alex Nichol, Casey Chu, and Mark Chen. Hierarchical text-conditional image generation with clip latents. *arXiv preprint arXiv:2204.06125*, 1(2):3, 2022. 2
- [37] Tal Reiss, Bar Cavia, and Yedid Hoshen. Detecting deepfakes without seeing any. *arXiv preprint arXiv:2311.01458*, 2023. 3
- [38] Robin Rombach, Andreas Blattmann, Dominik Lorenz, Patrick Esser, and Björn Ommer. High-resolution image synthesis with latent diffusion models. In *Proceedings of the IEEE/CVF conference on computer vision and pattern recognition*, pages 10684–10695, 2022. 1, 2, 15
- [39] Andreas Rossler, Davide Cozzolino, Luisa Verdoliva, Christian Riess, Justus Thies, and Matthias Nießner. Faceforensics++: Learning to detect manipulated facial images. In *Proceedings of the IEEE/CVF international conference on computer vision*, pages 1–11, 2019. 15
- [40] Chitwan Saharia, William Chan, Saurabh Saxena, Lala Li, Jay Whang, Emily L Denton, Kamyar Ghasemipour, Raphael Gontijo Lopes, Burcu Karagol Ayan, Tim Salimans, et al. Photorealistic text-to-image diffusion models with deep language understanding. *Advances in neural information processing systems*, 35:36479–36494, 2022. 2
- [41] Christoph Schuhmann, Richard Vencu, Romain Beaumont, Robert Kaczmarczyk, Clayton Mullis, Aarush Katta, Theo Coombes, Jenia Jitsev, and Aran Komatsuzaki. Laion-400m: Open dataset of clip-filtered 400 million image-text pairs. *arXiv preprint arXiv:2111.02114*, 2021. 15
- [42] Chuangchuang Tan, Yao Zhao, Shikui Wei, Guanghua Gu, Ping Liu, and Yunchao Wei. Rethinking the up-sampling operations in cnn-based generative network for generalizable deepfake detection. *arXiv preprint arXiv:2312.10461*, 2023. 3, 5, 6, 7, 8
- [43] Sheng-Yu Wang, Oliver Wang, Richard Zhang, Andrew Owens, and Alexei A Efros. Cnn-generated images are surprisingly easy to spot... for now. In *Proceedings of the IEEE/CVF conference on computer vision and pattern recognition*, pages 8695–8704, 2020. 2, 4, 5, 6, 7, 8, 9, 14

- [44] Zhendong Wang, Jianmin Bao, Wengang Zhou, Weilun Wang, Hezhen Hu, Hong Chen, and Houqiang Li. Dire for diffusion-generated image detection. In *Proceedings of the IEEE/CVF International Conference on Computer Vision*, pages 22445–22455, 2023. 3
- [45] World Economic Forum. The Global Risks Report 2024. https://www3.weforum.org/docs/WEF_The_Global_Risks_Report_2024.pdf, 2024. 1
- [46] Fisher Yu, Ari Seff, Yinda Zhang, Shuran Song, Thomas Funkhouser, and Jianxiong Xiao. Lsun: Construction of a large-scale image dataset using deep learning with humans in the loop. *arXiv preprint arXiv:1506.03365*, 2015. 5, 6, 14
- [47] Nan Zhong, Yiran Xu, Zhenxing Qian, and Xinpeng Zhang. Rich and poor texture contrast: A simple yet effective approach for ai-generated image detection. *arXiv preprint arXiv:2311.12397*, 2023. 3, 9
- [48] Jun-Yan Zhu, Taesung Park, Phillip Isola, and Alexei A Efros. Unpaired image-to-image translation using cycle-consistent adversarial networks. In *Proceedings of the IEEE international conference on computer vision*, pages 2223–2232, 2017. 2, 15
- [49] Mingjian Zhu, Hanting Chen, Qiangyu Yan, Xudong Huang, Guanyu Lin, Wei Li, Zhijun Tu, Hailin Hu, Jie Hu, and Yunhe Wang. Genimage: A million-scale benchmark for detecting ai-generated image. *Advances in Neural Information Processing Systems*, 36, 2024. 15
- [50] Bojia Zi, Minghao Chang, Jingjing Chen, Xingjun Ma, and Yu-Gang Jiang. Wildeeepfake: A challenging real-world dataset for deepfake detection. In *Proceedings of the 28th ACM international conference on multimedia*, pages 2382–2390, 2020. 15

9 Appendix

9.1 Architecture details

LaDeDa architecture. The LaDeDa architecture is almost identical to the ResNet50 architecture, except for a few changes in the convolutional layers kernel sizes, strides parameters, and the final fully connected layer. We describe the architecture used for 9×9 patch-size receptive field. LaDeDa follows the standard ResNet50 design with four main residual blocks (layer1, layer2, layer3, layer4) consisting of bottleneck residual units. The first convolutional layer has a kernel size of 1×1 and 64 output channels, followed by a 3×3 convolution with the same number of channels. The residual blocks employ bottleneck units with 1×1 convolutions for dimensionality reduction and expansion. The downsampling operation is a 1×1 convolution with stride 2. The number of channels increases from 64 in layer1 to 256, 512, 1024, and 2048 in subsequent layers. Layer1 consists of 3 parallel bottleneck units, layer2 has 4 parallel units, layer3 contains 6 parallel units, and layer4 has 3 parallel units. Layer2 is the last layers that uses a kernel size of 3 (the layers after uses a kernel size of 1), thus limiting the receptive field of the topmost convolutional layer. After layer4, a global average pooling operation is applied, followed by a fully connected layer with a single output neuron and a sigmoid activation function, for binary classification.

Tiny-LaDeDa architecture. The Tiny-LaDeDa architecture is a compact version of LaDeDa, designed for efficient performance with a reduced parameter count, using only 4 convolutional layers with 8 channels each. The architecture includes the following convolutional layers:

- 1×1 convolution (3 input channels, 8 output channels)
- 3×3 convolution (8 input channels, 8 output channels)
- 1×1 convolution (8 input channels, 8 output channels)
- 3×3 convolution (8 input channels, 8 output channels)

Tiny-LaDeDa results in a 5×5 receptive field. The final fully connected layer maps the 8 features to a single output, which is passed through a sigmoid activation function for binary classification. This streamlined architecture is lightweight and computationally efficient, making it suitable for real-time deepfake detection.

9.2 Implementation details

Training LaDeDa. To train LaDeDa, we use the Adam optimizer (26) with $\beta_1 = 0.9$, $\beta_2 = 0.999$, batch size 32 and initial learning rate of 2×10^{-4} . Learning rate is dropped by $10\times$ if after 5 epochs the validation accuracy does not increase by 0.1%, which is the same stopping criteria of (43; 32). During training, to have a uniform size, all images are resized to 256×256 resolution, and then randomly cropped to native size of 224×224 resolution. Note that we do not use post-processing augmentations (JPEG compression and Gaussian blur) as popular works (43; 32) do. During validation and test time, we directly resize the image to 256×256 resolution. As for the other baselines, we train them according to their official code repository. To train LaDeDa, we used a single NVIDIA RTX A5000 (21g).

Training Tiny-LaDeDa. To train Tiny-LaDeDa, we use LaDeDa’s patch-wise deepfake scores as soft labeling. We then use the Adam optimizer (26) with $\beta_1 = 0.9$, $\beta_2 = 0.999$, batch size of 729 (which is the number of 9×9 patches in an input image, and initial learning rate of 2×10^{-4} . To train Tiny-LaDeDa, we used a single NVIDIA RTX A5000 (21g).

9.3 Simulated protocol

9.3.1 Standard benchmarks in the simulated protocol

ForenSynth (43) and UFD (32) datasets. In this work, they chose ProGAN (24) as their single generative model in train set. Specifically, they used real images from LSUN (46), and fake images by train ProGAN on 20 different object categories of LSUN, and generate $18K$ fake images per category, resulting in $360K$ real and $360K$ fake images as the train set. As for the test set, they used ProGAN

(24), BigGAN (5), StyleGAN (25), GauGAN (33), CycleGAN (48), StarGAN (10), Deepfakes (39), SITD (7), SAN (12), IMLE (27), and CRN (8). Another work of (32) has suggested the **UFD** dataset, comprising variations of diffusion models: guided (15), GLIDE (31), LDM (38), and DALL-E (35) as the fake images. The real images sourced from the LAION (41) and ImageNet (13) datasets. In this work they also utilize the train set of the ForenSynth dataset to train their detector. By examining the dataset publication of LSUN (1) (the real images in the ForenSynth train set), we can see that all images have been resized to 256×256 resolution, and JPEG compressed with quality of 75. Additionally, the real images in the UFD datasets are also in JPEG format. In 5.1 we show that methods that use the train set of ForenSynth dataset, can become biased towards JPEG compression artifacts, when tested on a test set with the same biases.

GenImage Dataset (49) In this dataset, the real images are all the images in ImageNet (13). The fake images was generated using 100 distinct labels of ImageNet. The train set fake images were generated using Stable Diffusion V1.4 (38), and the test set fake images were generated using Stable Diffusion V1.4, V1.5 (38), GLIDE (31), VQDM (20), Wukong (3), BigGAN (5), ADM (15) and Midjourney (2). In total, GenImage contains 1, 331, 167 real and 1, 350, 000 fake images. However, also here, we can observe the preprocessing discrepancy mentioned above. ImageNet images (the real images in GenImage) are in JPEG format, while the generated images in GenImage saved in PNG.

9.3.2 Approaches for mitigating the datasets biases

A concurrent work of Grommelt et al. (19) showed that training a detector on GenImage can cause it functions as a JPEG detector. To overcome this discrepancy, the authors suggested using an unbiased GenImage dataset where the real and fake images have similar resolutions and are JPEG compressed with the same quality factor. Chai et al. (6) suggested to preprocess the images to make the real and fake dataset as similar as possible, in an effort to minimize the possibility of learning differences in preprocessing. To do so, they pass the real images through the data loading pipeline used to train the generator. As these approaches aim to mitigate the preprocessing differences between real and fake images, our approach uses images sampled from the distribution encountered in-the-wild, aiming to capture real-world artifacts differences between real and fake images.

9.4 Related datasets extracted from social networking platforms

Chen and Zou (9). In this work, they introduce a dataset of 800k ai-generated images with metadata from X (Twitter). However, the dataset is not opensourced and they did not provide real images, so we could not tested our method on it.

Zi et al. (50). In this work, they introduce a dataset comprising 7300 face sequences, with more persons in each scene, and more facial expressions, compared to other deepfakes videos datasets. The faces extracted from 700 deepfake videos collected from video-sharing websites. As we were not able to get access to this dataset, we could not tested our method on it.

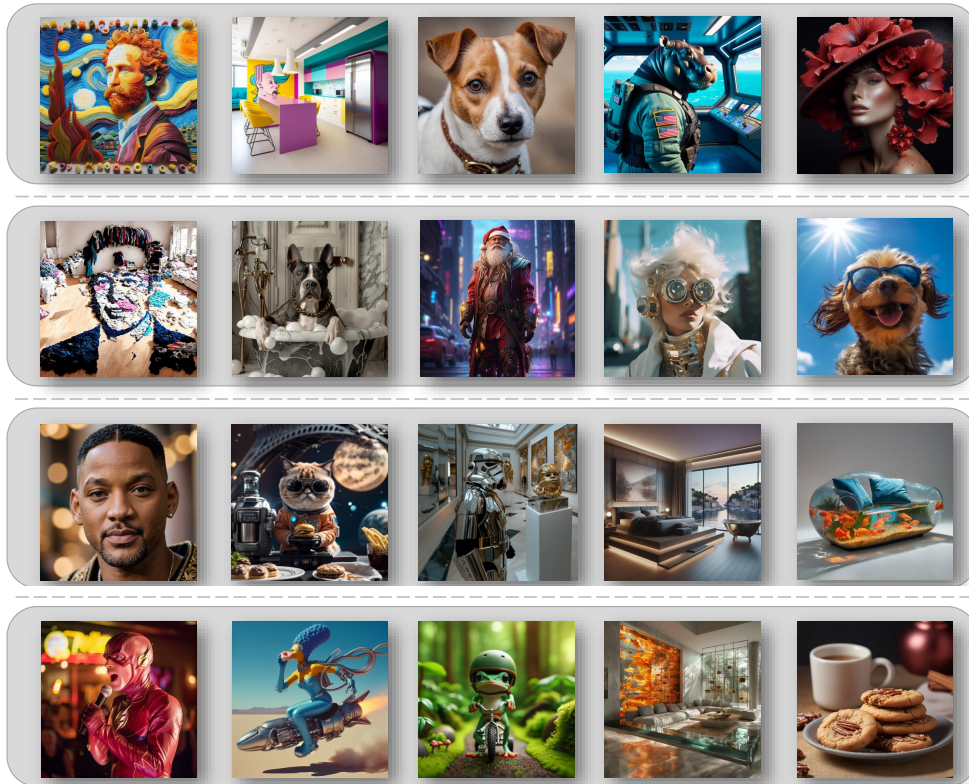


Figure 8: *Another WildRF image examples.*